

# Looking at structure, stability, and evolution of proteins through the principal eigenvector of contact matrices and hydrophobicity profiles

Ugo Bastolla,<sup>1</sup> Markus Porto,<sup>2</sup> H. Eduardo Roman,<sup>3,\*</sup> and Michele Vendruscolo<sup>4</sup>

<sup>1</sup>*Centro de Astrobiología (INTA-CSIC), 28850 Torrejón de Ardoz, Spain*

<sup>2</sup>*Institut für Festkörperphysik, Technische Universität Darmstadt, Hochschulstr. 8, 64289 Darmstadt, Germany*

<sup>3</sup>*Dipartimento di Fisica and INFN, Università di Milano, Via Celoria 16, 20133 Milano, Italy*

<sup>4</sup>*Department of Chemistry, University of Cambridge, Lensfield Road, Cambridge CB2 1EW, UK*

(Dated: October 31, 2018)

We review and further develop an analytical model that describes how thermodynamic constraints on the stability of the native state influence protein evolution in a site-specific manner. To this end, we represent both protein sequences and protein structures as vectors: Structures are represented by the principal eigenvector (PE) of the protein contact matrix, a quantity that resembles closely the effective connectivity of each site; Sequences are represented through the “interactivity” of each amino acid type, using novel parameters that are correlated with hydrophobicity scales. These interactivity parameters are more strongly correlated than the other hydrophobicity scales that we examine with: (1) The change upon mutations of the unfolding free energy of proteins with two-states thermodynamics; (2) Genomic properties as the genome-size and the genome-wide GC content; (3) The main eigenvectors of the substitution matrices. The evolutionary average of the interactivity vector correlates very strongly with the PE of a protein structure. Using this result, we derive an analytic expression for site-specific distributions of amino acids across protein families in the form of Boltzmann distributions whose “inverse temperature” is a function of the PE component. We show that our predictions are in agreement with site-specific amino acid distributions obtained from the Protein Data Bank, and we determine the mutational model that best fits the observed site-specific amino acid distributions. Interestingly, the optimal model almost minimizes the rate at which deleterious mutations are eliminated by natural selection.

## I. INTRODUCTION

The need to maintain the thermodynamic stability of the native state is an important determinant of protein evolution. This requirement has different effects on the various positions of the protein, depending on their structural environment. Therefore it is crucial to consider the effect of site-specific structural constraints in models of protein evolution, such as those used to estimate phylogenetic distances from the comparison of protein sequences (Nei and Kumar, 2000) or to reconstruct phylogenetic trees through Maximum Likelihood methods (Felsenstein, 1981).

The first and simplest models of this kind assumes a Gamma distribution of site-specific substitution rates (see Nei and Kumar, 2000). The Gamma distribution is flexible enough to interpolate between broad and narrow distributions, and its free parameter improves considerably the fit between models of evolution and multiple sequence alignments. Subsequently, site-specific amino acid frequencies (Halpern and Bruno, 1998) and site-specific substitution matrices determined for different structural classes (Liò and Goldman, 1998; Koshi and Goldstein, 1998; Koshi et al., 1999; Thorne, 2000; Parisi and Echave, 2001; Fornasari et al., 2002) were shown to further improve the reconstruction of phylogenetic trees. In these works, site-specificity is either empirically derived from the data or simulated with the help of some protein model. Following the latter approach, we recently showed that a structural property, the principal eigenvector (PE) of the contact matrix, is a strong predictor of site-specific amino acid conservation in models of protein evolution with stability con-

straints (Bastolla et al., 2004b).

We represent the amino acid sequence through a real-valued, site-specific profile, using the interactivity parameters derived by Bastolla et al. (2004b). The interactivity scale expresses the strength of effective interactions for each amino acid type, and its main component is the hydrophobicity. The interactivity parameters correlate more strongly than other hydrophobicity scales with thermodynamic quantities like the thermodynamic effect of a mutation, with genomic quantities such as the genome size and the genome-wide GC content in bacterial genomes, and with the main component of substitution matrices, as we discuss in the present paper.

By using the interactivity parameters and the PE as a structural indicator, we recently derived analytic expressions to predict site-specific amino acid distributions (Porto et al., 2004b). Amino acid distributions with a similar functional form have also been used previously by other authors (Koshi and Goldstein, 1998; Koshi et al. 1999; Dokholyan et al. 2001; 2002). Our predictions are in very good agreement with the distributions observed in the Protein Data Bank. Here we consider simple mutational models at the nucleotide level, and we show that they improve the fit between predicted and observed distributions. Interestingly, the mutational model that best fits the observed data is one for which deleterious mutations eliminated by negative selection appear with almost the lowest rate.

## II. MATERIALS AND METHODS

### A. Contact matrix and principal eigenvector

We represent a protein structure as a  $N \times N$  binary contact matrix  $C_{ij}$ , where  $N$  is the number of residues. The element  $C_{ij}$  is equal to one if amino acids  $i$  and  $j$  are in contact in the

\*Present address: Dipartimento di Fisica, Università di Milano Bicocca, Piazza della Scienza 3, 20126 Milano, Italy

native structure (i.e. at least one pair of their respective heavy atoms is closer than  $4.5 \text{ \AA}$ ), and zero otherwise. The contact matrix is symmetric, so it has  $N$  real eigenvalues. The PE is the eigenvector corresponding to the maximum eigenvalue and is indicated by  $\mathbf{c}$ . This vector maximizes the quadratic form  $\sum_{ij} C_{ij} c_i c_j$  with the constraint  $\sum_i c_i^2 = 1$ . In this sense,  $c_i$  can be interpreted as the effective connectivity of position  $i$ , since positions with large  $c_i$  are in contact with as many as possible positions  $j$  with large  $c_j$ . All its components have the same sign, which we choose by convention to be positive. Moreover, if the contact matrix represents a single connected graph (as for single-domain globular proteins), the information contained in the principal eigenvector is sufficient to reconstruct the whole contact matrix (Porto et al., 2004a). As we will review in this paper, the PE provides a convenient vectorial representation of a protein structure to be used in evolutionary studies.

### B. Free energy and interactivity parameters

The effective free energy for a sequence  $\mathbf{A}$  in configuration  $\mathbf{C}$  is estimated through an effective contact free energy function  $E(\mathbf{A}, \mathbf{C})$ ,

$$\frac{E(\mathbf{A}, \mathbf{C})}{k_B T} = \sum_{i < j} C_{ij} U(A_i, A_j), \quad (1)$$

where  $\mathbf{U}$  is a  $20 \times 20$  symmetric matrix whose element  $U(a, b)$  represents the effective interaction, in units of  $k_B T$ , of amino acids  $a$  and  $b$ ; we use the interaction matrix derived by Bastolla et al. (2001). For this interaction matrix the free energy function, Eq. (1), is lower for the native structure than for decoys generated by threading (Bastolla et al., 2001).

The effective energy function, Eq. (1), can be approximated through the main component of its spectral decomposition  $H(\mathbf{A}, \mathbf{C})$ ,

$$\frac{H(\mathbf{A}, \mathbf{C})}{k_B T} \equiv \varepsilon_1 \sum_{i < j} C_{ij} h(A_i) h(A_j). \quad (2)$$

where  $\varepsilon_1 < 0$  is the largest eigenvalue (in absolute value) of the matrix  $U(a, b)$  and  $h(a)$  is the corresponding eigenvector. The latter is mainly due to the contribution of hydrophobic interactions, as it is well known (Casari et al., 1992; Li et al., 1997). We therefore call the  $N$ -dimensional vector  $h(A_i)$  the Hydrophobicity Profile (HP) of sequence  $\mathbf{A}$  (Bastolla et al., 2004b). The 20 parameters  $h(a)$  obtained from the principal eigenvector of the interaction matrix are called *interactivity* parameters (IH). We will also use an optimized interactivity scale that was obtained by Bastolla et al. (2004b) by optimizing the correlation between the HP and the PE over a large set of proteins. Since the PE represents an effective connectivity, we indicate the latter scale with the abbreviation CH.

### C. Hydropathy scales

We consider eleven hydropathy scales, including the two interactivity scales described above. They are: (1) The KD

hydropathy scale, derived to identify trans-membrane helices using diverse experimental data (Kyte and Doolittle, 1982); (2) The L76 hydropathy scale, which was derived by using experimental data and theoretical calculations (Levitt, 1976); (3) The R88 hydropathy scale, which is based on the transfer of solutes from water to alkane solvents (Roseman, 1988); (4) The augmented Whilmey-White (WW) hydropathy scale, derived to improve recognition of trans-membrane helices (Jayasinghe et al., 2001); (5) The G98 classification of amino acids into polar, hydrophobic, and amphiphilic classes, adopted by Gu et al. (1998) to investigate the relationship between the hydrophobicity of a protein and the nucleotide composition of the corresponding gene; (6) The MP hydropathy scale, derived from statistical properties of globular proteins (Manavalan and Ponnuswamy, 1978); (7) The AV hydropathy scale derived by averaging 127 normalized hydropathy scales published in the literature (Palliser and Parry, 2001); (8) The FP hydropathy scale, derived from the experimental measurement of octanol/water partition coefficients (Fauchere and Pliska, 1983); (9) The Z04 scale, also called buriability, proposed by Zhou and Zhou (2004); (10) The interaction scale IH, obtained from the main eigenvector of the interaction matrix  $U(a, b)$  used in this work (Bastolla et al., 2004b); (11) The optimized interactivity scale, or connectivity scale CH, which maximizes the correlation with the principal eigenvectors of protein contact matrices for a non-redundant set of Protein Data Bank (PDB) structures (Bastolla et al., 2004b). All these scales have pairwise correlation coefficients ranging from a minimum of 0.68 (between the KD and L76 scales) to a maximum of 0.95 (between IH and CH scales).

### D. SCN model of neutral evolution

In the Structurally Constrained Neutral (SCN) model (Bastolla et al., 1999, 2002, 2003a, 2003b), starting from the protein sequence in the PDB, amino acid mutations are randomly proposed and accepted according to a stability criterion based on an effective model of protein folding (Bastolla et al., 2000, 2001). This ‘‘structural’’ approach has been pioneered by Schuster and co-workers, with a series of studies of neutral networks of RNA secondary structures (Schuster et al., 1994; Huynen et al., 1996; Fontana and Schuster, 1998) and it has been applied to proteins by several groups (Gutin et al., 1995; Bornberg-Bauer, 1997; Bornberg-Bauer and Chan, 1999; Babajide et al., 1997; Govindarajan and Goldstein, 1998; Bussemaker et al., 1997; Tiana et al., 1998; Mirny and Shakhnovich, 1998; Dokholyan and Shakhnovich, 2001; Parisi and Echave, 2001).

For testing the stability of a protein conformation, we use two computational parameters: (i) The effective energy per residue,  $E(\mathbf{A}, \mathbf{C})/N$ , Eq. (1), where  $N$  is the protein length. This quantity correlates with the folding free energy per residue for a set of 18 small proteins that are folding with two-states thermodynamics (correlation coefficient 0.91; U. Bastolla, unpublished result); (ii) The normalized energy gap  $\alpha$ , which characterizes fast folding model sequences (Bastolla et al., 1998) with well correlated energy landscapes (Bryngelson and Wolynes, 1987; Goldstein et al., 1992; Abkevich et al., 1994; Gutin et al., 1995; Klimov and Thirumalai, 1996). In

the SCN model, a mutated sequence is considered thermodynamically stable if both computational parameters are above predetermined thresholds (Bastolla et al., 2003a).

Simulations of the SCN model were performed for several protein folds. They all show the same two features: (1) After a very long evolutionary time, the protein sequence loses all recognizable similarity with the starting sequence, despite conserving the stability of its native fold. (2) Structural conservation varies across protein positions. The main structural determinant of evolutionary conservation is the principal eigenvector of the contact matrix.

### E. Site-specific distributions from the PDB

We obtain site-specific amino acid distributions from the PDB as follows. First, we select a non-redundant set of single-domain globular proteins, i.e. sequences with more than 90% homology with other chains in the PDB are excluded. A non-redundant list of proteins is given in the file `nrd90`, available at the PDB web site. Qualitatively equivalent results were obtained using the list selected with the method by Hobohm and Sanders (1994) with the much lower threshold of 25% sequence identity. Globular proteins are selected through the condition that the fraction of contacts per residue should be larger than a length-dependent threshold,  $N_c/N > 3.5 + 7.8N^{-1/3}$ . This functional form represents the scaling of the number of contacts in globular proteins as a function of chain length (the factor  $N^{-1/3}$  comes from the surface to volume ratio), and the two parameters are chosen so as to eliminate outliers with respect to the general trend, which are mainly non-globular structures. Single-domain proteins are selected by imposing the normalized variance of the PE components to be smaller than a threshold,  $(1 - N\langle c \rangle^2) / (N\langle c \rangle^2) < 1.5$ . Multi-domain proteins have large PE components inside their main domains and small components outside them. The PE components would be exactly zero outside the main domain if the domains do not form contacts. Therefore, multi-domain proteins are characterized by a larger normalized variance of PE components with respect to single-domain ones. The threshold of 1.5 eliminates most of the known multi-domain proteins and very few of the known single-domain proteins (data not shown).

The proteins are divided into groups according to their length. A first group comprises proteins with less than 100 amino acids and contains about  $8 \times 10^3$  sites. A second group comprises proteins of length between 101 and 200 amino acids and contains  $5.2 \times 10^4$  sites. These two groups are joined to improve the statistics in cases where we are not interested in length dependence. A third group comprises proteins with length between 201 and 400 amino acids and contains  $6 \times 10^5$  sites. Within each group, sites are divided in structural classes depending on the value of their normalized PE component,  $c_i/\langle c \rangle$ , using a bin width of 0.1. For each structural class, the distribution of the 20 types of amino acids is obtained. We refer to this distribution with the symbol  $\pi_{c_i/\langle c \rangle}^{\text{PDB}}(a)$ , where  $a$  indicates one of the 20 types of amino acids.

### F. Distance measures for amino acid distributions

The Jensen-Shannon divergence of two given distributions  $P(a)$  and  $Q(a)$  is defined as

$$D_{\text{JS}}(P, Q) = \frac{1}{2} \sum_a \left[ P(a) \log_2 \left( \frac{P(a)}{R(a)} \right) + Q(a) \log_2 \left( \frac{Q(a)}{R(a)} \right) \right], \quad (3)$$

where  $R(a) = [P(a) + Q(a)]/2$ . This measure is equivalent to the difference of the entropy of the ‘average distribution’  $R$  minus the average entropy of distributions  $P$  and  $Q$ . It is positive, symmetric, and takes values between zero and one.

This information-theoretical distance measure, however, does not take into account the physico-chemical similarities between amino acids. In the present context, it is natural to focus our attention on the amino acid interactivity  $h(a)$ , which determines the predicted site-specific distributions. Predicted distributions are defined imposing the value of their first moment, so it is natural to define the  $D_{h^2}$  distance as the squared difference between the second moments

$$D_{h^2}(P, Q) = \left\{ \frac{1}{20} \sum_a h^2(a) [P(a) - Q(a)] \right\}^2 \equiv ([h^2]_P - [h^2]_Q)^2. \quad (4)$$

We average the distance measures between observed and predicted distributions for different values of the structural parameter  $c_i/\langle c \rangle$ . In the case of the  $D_{h^2}$  distance, we normalize this measure in order to reduce its dependence on the scale of the hydrophobicity parameters. We choose the normalization

$$D_{h^2}(P, Q) = \frac{\langle ([h_i^2]_P - [h_i^2]_Q)^2 \rangle_i}{\langle [h_i^2]_P \rangle_i \langle [h_i^2]_Q \rangle_i}, \quad (5)$$

where angular brackets define the average over positions  $i$ .

### G. Substitution matrix

The procedure described by Henikoff and Henikoff (1992) for calculating substitution matrices starts by generating a multiple sequence alignment and counting the amino acid distribution at each position,  $\pi_i^{\text{ali}}(a)$ . For large number of aligned positions, the logarithm of odds matrix that they define can be approximated as

$$S_{ab} = \log \left[ \frac{\langle \pi_i^{\text{ali}}(a) \pi_i^{\text{ali}}(b) \rangle_i}{\langle \pi_i^{\text{ali}}(a) \rangle_i \langle \pi_i^{\text{ali}}(b) \rangle_i} \right], \quad (6)$$

where the angular brackets indicate an average over aligned positions  $i$ .

Using Eq. (6), we calculate the substitution matrix generated by aligning positions of proteins in the PDB having the same value of the normalized PE,  $c_i/\langle c \rangle$ , in an interval of width 0.1.

## H. Normalized matrix decomposition

Usually, the eigenvectors  $\mathbf{v}^{(\alpha)}$  of a  $N \times N$  symmetric matrix  $M_{ij}$  are normalized such that their squared components sum to one,  $\sum_i (v_i^{(\alpha)})^2 = 1$ . In this case, the spectral decomposition of the matrix can be expressed as

$$M_{ij} = \sum_{\alpha} \lambda_{\alpha} v_i^{(\alpha)} v_j^{(\alpha)}. \quad (7)$$

The relative importance of each eigenvector, however, does not only depend on the corresponding eigenvalue  $\lambda_{\alpha}$ , but also on the average eigenvector component. To make this dependence more explicit, it is convenient to transform the eigenvectors in such a way that their average component is zero and their variance is one, *i.e.* by defining new vectors  $\eta_i^{(\alpha)} = (v_i^{(\alpha)} - \langle v^{(\alpha)} \rangle) / \sqrt{N^{-1} - \langle v^{(\alpha)} \rangle^2}$ . The spectral decomposition now reads

$$M_{ij} = \frac{1}{N} \sum_{\alpha} \lambda_{\alpha} \left[ w_{\alpha} + \sqrt{w_{\alpha} - w_{\alpha}^2} (\eta_i^{(\alpha)} + \eta_j^{(\alpha)}) + (1 - w_{\alpha}) \eta_i^{(\alpha)} \eta_j^{(\alpha)} \right], \quad (8)$$

where  $w_{\alpha} = N \langle v^{(\alpha)} \rangle^2$ . These satisfy the normalization  $\sum_{\alpha} w_{\alpha} = 1$ . The first term in the square brackets is the same for all pairs  $i$  and  $j$ . The second term is proportional to the sum of the normalized eigenvector components, and the third term is proportional to their product. Therefore, we define two combinations of the eigenvalues and the mean eigenvector components as

$$\ell_{\alpha}^{\text{sum}} = \frac{\lambda_{\alpha} \sqrt{w_{\alpha} - w_{\alpha}^2}}{\sum_{\beta} \lambda_{\beta} w_{\beta}} \quad (9a)$$

and

$$\ell_{\alpha}^{\text{prod}} = \frac{\lambda_{\alpha} (1 - w_{\alpha})}{\sum_{\beta} \lambda_{\beta} w_{\beta}}. \quad (9b)$$

## III. RESULTS AND DISCUSSION

### A. Interactivity and folding thermodynamics

It is well known that hydrophobicity is one of the main determinants of protein thermodynamics. Gromiha et al. (1999) showed that properties reflecting hydrophobicity correlate with the stability of buried mutations. We tested the ability of various hydrophobicity scales to predict the average effect of single amino acid mutations (Bastolla, unpublished).

We use a database of more than  $10^3$  mutants, selected by Guerois et al. (2002). We average the change in folding free energy for each amino acid substitution present in this database with more than four examples. These average changes are correlated with the difference of hydrophobicity parameters for various hydrophobicity scales. The rationale for testing these correlations is that, from Eq. (2), it follows that

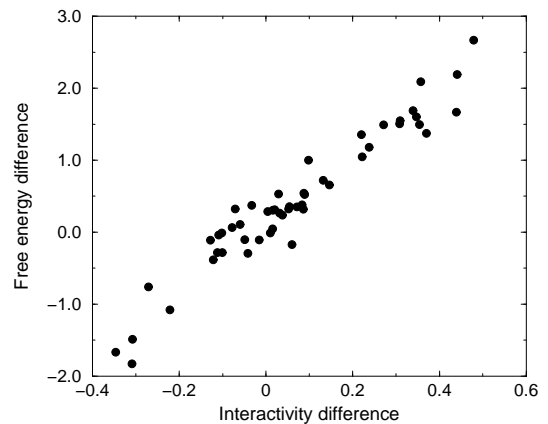


FIG. 1: Comparison between the difference of interactivity parameters and the average free energy difference upon mutation for amino acid pairs for which sufficient mutations have been studied. The correlation coefficient is  $R = 0.87$ .

the difference between the effective unfolding free energy of a protein mutated at position  $i$  and the wild-type is proportional to  $\Delta\Delta G \propto [h(A_i^{\text{wt}}) - h(A_i^{\text{mut}})] \sum_j C_{ij} h(A_j)$ .

All hydrophobicity scales that we use are correlated with the average changes in the folding free energy. The strongest correlation is found for the improved interactivity parameters CH, represented in Fig. 1. They provide better predictions than all the other parameters that we examined (see Table I).

The influence of hydrophobicity on protein stability is complex. A more interactive protein tends to have larger unfolding free energy, so that it is more stable with respect to unfolding. However, alternative compact configurations also have lower free energies, so that the normalized energy gap is smaller and the protein may be less stable with respect to misfolding.

This qualitative picture is supported by a computational study of folding thermodynamics in families of orthologous proteins with the same structure and function expressed in different prokaryotic organisms (Bastolla et al., 2004a). That study found a positive correlation between the mean hydrophobicity and the predicted unfolding free energy, and a negative correlation between hydrophobicity and the normalized energy gap. The correlations hold qualitatively for all the hydrophobicity scales examined in this study. The strongest correlations are found for the optimized interactivity parameters CH, whereas the weakest ones are found for the KD parameters (see Table I).

A strong influence of hydrophobicity on protein folding thermodynamics was also found in a recent statistical analysis of experimental results: Proteins which are only weakly hydrophobic are unable to fold, *i.e.* they are ‘natively unfolded’ (Uversky, 2002a), whereas strongly hydrophobic proteins are often characterized by folding intermediates (Uversky, 2002b), which in some cases slow down the folding process and increase the risk of misfolding. Interestingly, such very hydrophobic proteins are found more frequently in obligatorily intracellular bacteria (Bastolla et al., 2004a), whose effective population size is small due to the bottlenecks during transmission to new hosts, so that natural selection is less effective in their evolution (Ohta, 1976). These bacteria have a

hydrophobicity scale	$C(h, \Delta\Delta G)$	$C(h, \alpha)$	$C(h, \Delta G/N)$	$C(h, GC_{12})$	$C(h, \text{genome size})$	$C(h, s_{25})$	$C(h, s_{\text{Blosum}})$	$C(h, s_{\text{PE}})$	$C(h, \text{PE})$
KD	0.43	-0.37	0.22	-0.14	-0.16	-0.76	-0.82	0.74	0.990
L76	0.53	-0.35	0.35	-0.20	-0.23	-0.82	-0.82	0.77	0.992
R88	0.55	-0.39	0.32	-0.32	-0.27	-0.78	-0.82	0.74	0.993
WW	0.63	-0.46	0.49	-0.34	-0.35	-0.85	-0.86	0.81	0.994
G98	0.66	-0.61	0.54	-0.48	-0.48	-0.87	-0.92	0.83	0.993
MP	0.67	-0.45	0.67	-0.32	-0.38	-0.90	-0.91	0.89	0.990
AV	0.72	-0.58	0.58	-0.40	-0.41	-0.95	-0.96	0.93	0.994
FP	0.77	-0.52	0.57	-0.42	-0.42	-0.92	-0.94	0.90	0.994
Z04	0.80	-0.67	0.71	-0.47	-0.50	-0.96	-0.96	0.97	0.994
IH	0.78	-0.68	0.83	-0.59	-0.55	-0.94	-0.94	0.94	0.994
CH	0.87	-0.72	0.83	-0.72	-0.61	-0.97	-0.95	0.98	0.995

TABLE I: Correlation coefficients calculated for various hydrophobicity scales. Column 2: Changes in hydrophobicity and average change in unfolding free energy upon mutation; Columns 3 to 6: Average hydrophobicity of proteins in bacterial genomes and: Average normalized energy gap (column 3), predicted unfolding free energy (column 4), GC content in first plus second codon positions (column 5), and genome size (column 6); Column 7 to 9: Hydrophobicity parameters and the main eigenvector of three substitution matrices: column 7: Matrix derived by Kinjo and Nishikawa (2004) from aligned proteins with 25% sequence identity (other matrices by the same authors give essentially the same results); column 8: The Blosum matrix (Henikoff and Henikoff, 1992); column 9: The matrix obtained from PE alignments (this work). Column 10: Correlation between the PE and the average HP for each PE class.

very high expression level of molecular chaperones, i.e. proteins that assist the folding of other proteins and reduce the negative effects of misfolding (Hartl and Hayer-Hartl, 2002). Therefore, it is possible that the large hydrophobicity observed in these proteins is, at least in part, a consequence of the reduced efficiency of natural selection, which has to be compensated through overexpression of chaperones (Fares et al., 2004).

Possibly as a consequence of this trade-off on folding thermodynamics (Bastolla et al., 2004a), the mean hydrophobicity of globular proteins has a rather narrow distribution. However, for the same reason, small variations of hydrophobicity close to the maximum of the distribution are expected to have only a weak effect on protein folding efficiency, since they tend to be favorable for one property but unfavorable for the other property. This might be the reason why the GC content at first and second codon positions, which strongly influences the interactivity of orthologous proteins (see below), is strongly correlated with the GC content at the third, often synonymous, codon position (Sueoka, 1961; Bernardi and Bernardi, 1986; Lobry, 1997), which, on a genome-wide basis, is thought to reflect the mutational bias.

## B. Interactivity and genomic quantities

Two important features in bacterial genomes, genome size and mean GC content of protein coding genes, have a negative correlation with the average interactivity of proteins expressed in those genomes, as compared with the orthologous proteins expressed in other organisms (Bastolla et al., 2004a). Small bacterial genomes with low GC genes (two properties that tend to go together in prokaryotic organisms) lead to proteins of higher hydrophobicity. We find that the optimized interactivity parameters CH have the strongest correlations among all hydrophobicity scales that we considered, whereas the KD scale has lowest and non-significant correlations (see Table I).

The relationship between hydrophobicity and GC content is due to the structure of the genetic code. As noted by several authors, Thymine in the second codon position is almost always associated with hydrophobic amino acids. In this respect, the low correlation found between the KD hydrophobicity scale and both genomic and thermodynamic quantities is explained by the fact that this scale attributes small or negative hydrophobicity to aromatic amino acids (Phe, Trp, Tyr), which have large interactivity values and are AT rich in their codons.

The relationship between hydrophobicity and prokaryotic genome size can be attributed in part to mutation, since bacteria with small genomes tend to have mutational bias towards AT, and in part to selection. Indeed, bacteria with small genomes usually have an intracellular lifestyle, which implies reduced effective populations and reduced efficiency of natural selection. This interpretation, which we mentioned above, is supported by the observation that the GC content at the first and second codon positions appears to be more influenced by the mutationally driven GC content at third position in low GC intracellular bacteria than in free living bacteria with intermediate GC in their large genomes, indicating that negative selection is less efficient despite the fact that the effects of very low GC on protein folding thermodynamics are expected to be severe (Bastolla et al., 2004a).

## C. Optimal Hydrophobicity Profile

Several analytic insights into protein folding and evolution can be derived from Eq. (2). First, the contact matrix whose PE is parallel to the HP minimizes Eq. (2) for a fixed value of the principal eigenvalue. However, usually there is no protein structure that satisfies the constraints of chain connectivity, excluded volume, and hydrogen bonding and possesses the optimal contact matrix, so that minimization of Eq. (2) in the space of allowed protein structures can not be performed

analytically. Second, we can define the optimal HP of a contact matrix,  $\mathbf{h}_{\text{opt}}$ , as the HP that minimizes the approximate effective free energy, Eq. (2), for fixed first and second moment of the hydrophobicity vector,  $\langle h \rangle = N^{-1} \sum_i h(A_i)$  and  $\langle h^2 \rangle = N^{-1} \sum_i h(A_i)^2$ . It is easy to see that the optimal HP so defined, is very strongly correlated with the PE (Bastolla et al., 2004b).

The condition on the mean hydrophobicity,  $\langle h \rangle$ , is imposed because, if a sequence is highly hydrophobic, not only the native structure but also alternative compact structures will have favorable hydrophobic energy. Selection to maintain a large normalized energy gap is therefore expected to limit the value of  $\langle h \rangle$ , and indeed this quantity is narrowly distributed in globular proteins. The optimal HP constitutes an analytic solution to the sequence design problem with energy function given by Eq. (2), and an approximate solution to sequence design with the full contact energy function, Eq. (1).

In the SCN evolutionary model, attempted mutations are accepted when the effective free energy and the normalized energy gap exceed predefined thresholds. Therefore, we do not expect the optimal HP to be ever observed during evolution, but we do expect thermodynamically stable sequences compatible with a given fold to have HPs distributed around the optimal one, and therefore correlated with the corresponding PE.

The above prediction is in agreement with simulations of the SCN model. The PE of a protein fold is significantly correlated with the HPs of its individual SCN sequences (the mean correlation coefficient is 0.45, averaged over seven proteins and hundred thousands simulated sequences per protein), and very strongly correlated with the average HP of all its sequences. The result of this average is indicated by the symbol  $[h_i]_{\text{evol}}$ , since it represents an effective evolutionary average. Its mean correlation coefficient with the PE is 0.96, averaged over the same seven folds (Bastolla et al., 2004b).

Thus we can almost recover the optimal HP through an evolutionary average of the HPs compatible with the protein fold. Assuming that the correlation coefficient between the PE and the average HP is exactly one, as in the case of the SCN model, we can predict average HP as (Porto et al., 2004b)

$$[h_i]_{\text{evol}} \equiv \sum_{\{a\}} \pi_i(a) h(a) = A (c_i / \langle c \rangle - 1) + B, \quad (10)$$

where the sum over  $\{a\}$  is over all amino acids, and

$$A = \sqrt{\frac{\langle [h]_{\text{evol}}^2 \rangle - \langle [h]_{\text{evol}} \rangle^2}{(\langle c^2 \rangle - \langle c \rangle^2) / \langle c \rangle^2}} \quad (11a)$$

and

$$B = \langle [h]_{\text{evol}} \rangle. \quad (11b)$$

For protein families represented in the PFAM (Bateman et al., 2000) and in the FSSP (Holm and Sander, 1996) databases the PE is significantly correlated with the HP of individual sequences. In this case, however, the correlation between the PE components and  $[h_i]_{\text{evol}}$  is considerably weaker: The mean correlation coefficient is 0.57 for PFAM families and 0.58 for FSSP families (Bastolla et al., 2004b). This weaker

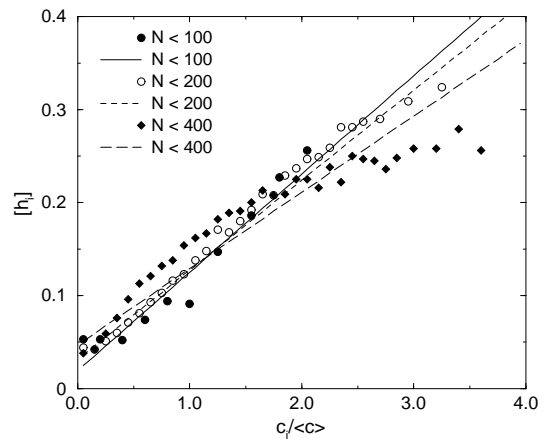


FIG. 2: Site-specific mean hydrophobicities as a function of the corresponding normalized PE components for proteins of three different length classes. The lines indicate the theoretical predictions, Eq. (10).

correlation is not unexpected, since functional conservation is not accounted for in the SCN model, and the effective energy function on which the interactivity is based is only an approximation. In addition, the number of sequences used to calculate the average HP of PFAM and FSSP families is much smaller than the number of SCN sequences considered. When  $[h_i]_{\text{evol}}$  is computed from only a few hundred SCN sequences, as in PFAM or FSSP families, the correlation with the PE also drops considerably.

We overcome these limitations by considering structural alignments of PDB proteins based on the PE. This eliminates conservation due to functional constraints and increases the sample size with respect to sequence based alignments. In our prediction, the normalized PE component at site  $i$ ,  $c_i / \langle c \rangle$ , determines the average hydrophobicity at that site. Therefore, we average together hydrophobicities at sites with similar normalized PE components in a narrow range (see Materials and Methods). The average HPs correlate very strongly with the PE, with correlation coefficients very close to one for all hydrophobicity scales (see Table I). The average values are compared in Fig. 2 to the values predicted through Eq. (10). It is apparent from this figure that the prediction must be corrected for high PE components, where the hydrophobicity values are close to the maximum of the hydrophobicity scale.

Fig. 2 also shows that the slope of the predicted lines, expressing the dependence of  $[h_i]_{\text{evol}}$  on the PE component, becomes smaller for longer proteins. According to Eqs. (10,11a), this happens because the standard deviation (and also the mean) of the hydrophobicity profile decreases for longer proteins. From Fig. 2 we also notice that the discrepancy between predicted and observed  $[h_i]_{\text{evol}}$  increases for longer proteins. Consistently, we observe that longer proteins have a weaker correlation between their PEs and HPs. These results suggest that the selection for proper hydrophobicity is less stringent for longer proteins (Porto et al., 2004b), consistently with the observation that longer proteins have more native interactions per residue, and these tend to be weaker and less optimized with respect to non-native interactions (Bas-

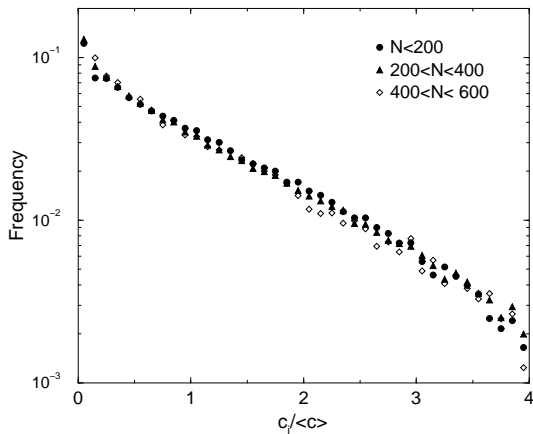


FIG. 3: Distribution of the normalized PE components,  $c_i / \langle c \rangle$ .

tolla and Demetrius, 2004).

The normalized PE components,  $c_i / \langle c \rangle$ , are distributed exponentially, as shown in Fig. 3. Therefore, larger PE components are less frequently found in protein structures.

#### D. Site-specific amino acid distributions

The PE and the HP also allow site-specific amino acid distributions to be predicted. We hypothesize that the mean hydrophobicity, Eq. (10), is the only condition that the site-specific amino acid distributions have to fulfill. Consequently, we assume that these distributions maximize the entropy for a fixed value of  $[h_i]_{\text{evol}}$ . It immediately follows that the resulting distributions have the form

$$\pi_i(a) \propto \exp[-\beta_i h(a)], \quad (12)$$

where the site-specific Boltzmann parameters (‘inverse temperature’)  $\beta_i$  determine the width of the distribution and can be obtained inverting Eq. (10). These distributions so obtained are in very good agreement with the site-specific amino acid distributions obtained by simulating the SCN model, as well as with empirical distributions obtained from the PDB (Porto, 2004b).

Site-specific amino acid distributions with a Boltzmann form, similar to those obtained above, have been used in other studies of protein evolution. Koshi and Goldstein (1998) and Koshi et al. (1999) assumed Boltzmann distributions of physico-chemical amino acid properties, and fitted their parameters from sequence alignments using the Maximum Likelihood method. Dokholyan et al. (2001; 2002) obtained similar distributions as a mean-field approximation of a model of protein design and evolution. Also in this case the parameters of the distributions were obtained from protein alignments. A main difference between these previous models and our approach is that the latter allows to compute analytically the Boltzmann parameters, without the need of a fitting on a database.

Despite the good agreement with observations, our approach is neglecting a very important element, namely the mutation process acting at the DNA level. Protein evolution takes

place by mutation, which acts on individual proteins, and by fixation of a mutant protein, which is a population-level process. We assume here that the time scale for the appearance of new mutations is longer than the time scale for their fixation of the population, which is the case when the product of the effective population size  $M$  times the mutation frequency  $\mu$  is smaller than one. This assumption is appropriate for animal populations, but it is incorrect for RNA-virus populations, and possibly for some very large bacterial populations.

We represent protein evolution as an effective stochastic process with a transition matrix

$$T(a, b) = P_\mu(a, b) P_{\text{fix}}(a, b) \quad (13)$$

for a substitution from  $a$  to  $b \neq a$ . The first factor represents the mutation process and the second one represents the neutral fixation of mutations that conserve thermodynamic stability. Our results for the SCN model show that, for what concerns the stationary distribution, the fixation term can be written as

$$P_{\text{fix}}(a, b) = \min\{1, \exp(-\beta_i [h(b) - h(a)])\}, \quad (14)$$

where the Boltzmann parameter  $\beta_i$  takes the value that fulfills Eq. (10). Notice that, the larger is the absolute value of  $\beta_i$ , the larger is the fraction of mutations which are eliminated by negative selection for protein stability and the larger is the mutational load.

The stationary distribution of the complete transition matrix has the form  $\pi(a, \beta) \propto \exp[-\beta h(a)] w_\beta(a)$ , where  $w_\beta(a)$  satisfies the equations

$$0 = \sum_{a \neq b} \min\{\exp[-\beta h(b)], \exp[-\beta h(a)]\} \times [w_\beta(a) P_\mu(a, b) - w_\beta(b) P_\mu(b, a)], \quad (15)$$

for all final amino acid states  $b$ . If the mutation matrix satisfies the detailed balance equation,  $w(a) P_\mu(a, b) = w(b) P_\mu(b, a)$ , then the stationary distribution of the mutation plus fixation process has the form

$$\pi_i(a) = \frac{w(a) \exp[-\beta_i h(a)]}{\sum_{a'} w(a') \exp[-\beta_i h(a')]}, \quad (16)$$

where  $w(a)$  is the stationary distribution of the mutation process, which is also the stationary distribution of the protein evolution process at sites where  $\beta_i$  equals zero (no rejection of mutations).

We use the simplifying hypothesis of Eq. (16) and adopt three different models for obtaining the weights  $w(a)$ . These models are scored by comparing predicted and observed distributions through the Jensen-Shannon (JS) and  $h^2$  distance measures,  $D_{JS}$  and  $D_{h^2}$  (see Materials and Methods). The optimized (CH) and diagonalized interactivity scales (IH) provide the best matches between observed and predicted distributions in terms of JS distance in almost all studied cases. The next best match is provided by the buriability (Z04) scale. In the following, the results presented refer to the CH interactivity scale.

We consider for comparison a model with  $w(a) \equiv 1$ , which corresponds to  $P_\mu(a, b) = 1/20$ . This is the mutational model that we adopt in the SCN simulations. Surprisingly, this simple model provides already rather good predictions for amino

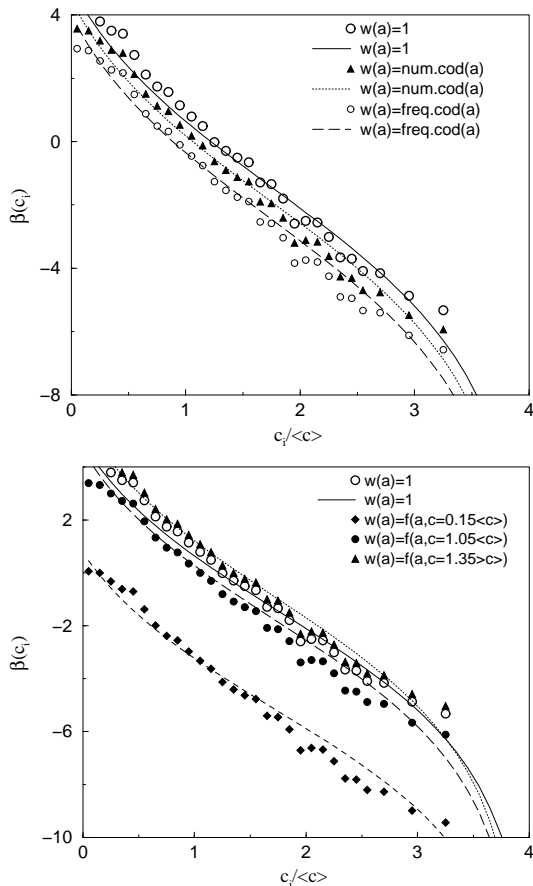


FIG. 4: Boltzmann parameters of site-specific distributions for different choices of  $w(a)$ . Upper panel:  $w(a)$  from number of codons and optimal codon frequency. Lower panel:  $w(a) = f(a, c)$  at  $c/\langle c \rangle = 0.15, 1.05, \text{ and } 1.35$ .

acid distributions (Porto et al., 2004b). The average JS divergence between predicted and observed frequencies in the PDB is  $D_{JS} = 0.0294$  (see Table II).

In order to formulate an improved model, we choose at first  $w(a)$  to be proportional to the number of codons coding for the amino acid  $a$ , see Fig. 4a. This choice improves by almost 40% the  $D_{JS}$  distance, but it has little effect on the  $D_{h^2}$  distance.

Secondly, we consider that not only the number of codons, but also the nucleotide frequency influences the amino acid frequency. We adopt therefore the expression

$$w(a) \propto \sum_{\text{codons}(a)} f(n_1) f(n_2) f(n_3), \quad (17)$$

where  $f(n)$  is the frequency of the four nucleotides A, T, G, and C. The previous ansatz based on the number of codons is equivalent to assuming identical frequencies for the four nucleotides. The nucleotide frequencies providing the optimal match are found by enumeration of all combinations in a reasonable range, with discretization step of 0.005. For the IH intractivity parameters, the optimal frequencies are T = 0.240, C = 0.195, A = 0.310, and G = 0.255. These frequencies are close to observed nucleotide frequencies in protein coding genes, and they do not change much when we use other

$w(a)$	$D_{JS}$	$D_{h^2}$	$D_{\beta}$	$\langle  \beta_i  \rangle$
constant	0.0294	0.338	0.128	0.416
number of codons	0.0247	0.282	0.136	0.388
optimal codon frequency	0.0172	0.271	0.129	0.362
uniform codon mutations	0.0256	0.285	0.256	0.393
frequency at $c = 1.05 \langle c \rangle$	0.0087	0.265	0.177	0.380

TABLE II: Distances and average absolute Boltzmann parameter for distributions obtained for various models of  $w(a)$ .

hydropathy scales, or the  $D_{h^2}$  measure instead of  $D_{JS}$ . The improvement in  $D_{JS}$  is a further 30%, but the improvement in  $D_{h^2}$  is modest.

The third approach considers that, for  $\beta = 0$ , the expected amino acid frequencies coincide with the weights  $w(a)$ . We therefore obtain  $w(a)$  parameters from the frequencies observed at various values of  $c/\langle c \rangle$ , where we effectively set  $\beta = 0$ , see Fig. 4b. Note that this approach requires to obtain 19 additional parameters from the data and it does not correspond to any mutational model. Therefore, the fact that it better fits the data is not significant, and we show these results only for comparison. In this case the improvement of the  $D_{JS}$  measure is dramatic, as expected, for  $c/\langle c \rangle$  in the range between zero and two. The  $D_{h^2}$  measure improves only modestly, and it becomes worse for  $c/\langle c \rangle > 1.2$ . The combination of the two criteria and the comparison of  $\beta$  values from observed and predicted distributions favour weights derived at  $c/\langle c \rangle$  between zero and one. Notice however that, if  $c/\langle c \rangle$  is much smaller than one, meaning that we fit the weight at positions with small PE component, the required  $\beta$  parameters are much more negative. This fact can be interpreted as a strong selective pressure acting on positions with large PE component.

Lastly, we solve Eq. (15) numerically for a mutation matrix obtained by considering all nucleotide mutations as equiprobable. This process has a stationary distribution that is almost proportional to the number of codons of each amino acid. Accordingly, its prediction coincides almost perfectly with the one obtained by choosing  $w(a)$  proportional to the number of codons, even if detailed balance is not assumed. This result justifies the approximation of considering matrices that satisfy detailed balance. Results corresponding to various models are summarized in Table II.

### E. Rejection rate

Using the mutation matrix  $P_{\mu}(a, b)$  and the fixation probability Eq. (14), we can compute the equilibrium fraction of mutations which are eliminated by negative selection at site  $i$  with Boltzmann parameter  $\beta$  (we omit the index  $i$  for simplicity),

$$P_{\text{rej}}(\beta) = \sum_{a=1}^{20} \sum_{\substack{b \text{ with} \\ \beta h(a) < \beta h(b)}} w_{\beta}(a) P_{\mu}(a, b) \times (e^{-\beta h(a)} - e^{-\beta h(b)}). \quad (18)$$



The computation of this quantity requires to know the mutation matrix, whereas our assumption of detailed balance only requires to specify the stationary nucleotides frequencies under no selection ( $\beta = 0$ ). Therefore, we evaluate the rejection rate through the average of the absolute value of the Boltzmann parameters  $\langle |\beta_i| \rangle$ .

Among the models that we considered,  $\langle |\beta_i| \rangle$  is lowest for the more elaborate model taking into account nucleotide frequencies. Among all possible nucleotide frequencies, the lowest value of  $\langle |\beta_i| \rangle$  is 0.348, and it is attained at nucleotide frequencies close to those giving the optimal fit,  $T = 0.200$ ,  $A = 0.320$ ,  $C = 0.180$ , and  $G = 0.300$ . Even lower values of  $\langle |\beta_i| \rangle$  and better fits can be obtained deriving the  $w(a)$  from the amino acid frequencies observed at specific values of the PE component (the minimum value of  $\langle |\beta_i| \rangle$  is 0.328, attained when the  $w(a)$  coincide with the frequencies observed at  $c_i = 0.75 \langle c \rangle$ ), but these values are ad-hoc since they are not the result of a mutational model. These results suggest that mutation frequencies are set to almost optimize the mutational load.

#### F. Interactivity and substitution matrices

Kinjo and Nishikawa (2004) recently calculated substitution matrices derived from protein alignments with various values of the sequence identity of the aligned proteins. Qualitatively, these substitution matrices measure the tendency of two residue of types  $a$  and  $b$  to co-occur at aligned sites. Kinjo and Nishikawa noticed that the eigenvector corresponding to the largest positive eigenvalue of the substitution matrices is correlated with the hydrophobicity, and that the corresponding eigenvalue increases with decreasing sequence alignment, corresponding to longer evolutionary time.

We examine the substitution matrices calculated by Kinjo and Nishikawa for various sequence identities, and we consider for comparison the matrix Blosum62 (Henikoff and Henikoff, 1992). We also obtain a new substitution matrix from the alignment of PDB structures based on the normalized PE components, as described in Materials and Methods. This latter substitution matrix can also be predicted analytically using the formulas for site-specific distributions given above. Its non-diagonal elements are correlated with the corresponding elements of the Blosum62 matrix, with  $R = 0.66$ . However its diagonal elements are much smaller than the corresponding Blosum elements, since all 20 amino acids can be found with fairly large frequencies at each aligned position.

We calculate the correlation of the eigenvector corresponding to the largest positive eigenvalue of these substitution matrices with the hydrophobicity scales described in Materials and Methods. For almost all matrices, the largest correlation (with  $R = -0.95$  to  $-0.97$ ) is found for the optimized interactivity parameters, but the correlation is very high also for other scales, see Table I.

We then computed the normalized eigenvalue of this eigenvector, Eq. (9b). From its behavior as a function of sequence identity (see Fig. 5) one sees that the contribution of the hydrophobicity to the substitution matrices becomes more important for lower identities of the aligned proteins, *i.e.* for increased evolutionary time. The Blosum matrix corresponds

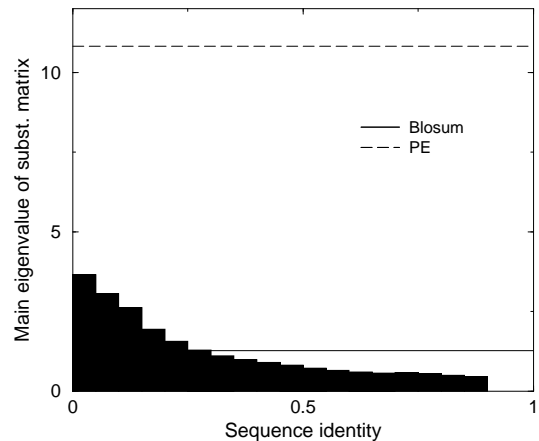


FIG. 5: Normalized eigenvalue corresponding to the hydrophobicity contribution to substitution matrices as a function of the sequence identity used to derive the matrix. The Blosum matrix and the matrix derived from PE-based alignment are also shown.

to an intermediate value, whereas the matrix obtained from aligned PDB structure is completely dominated by hydrophobicity, as expected from Eq. (6). This matrix corresponds to the limit of very long evolutionary time, where all sequence similarity is lost, apart for that originated by the common structural environment expressed by the PE. Therefore, this study of substitution matrices further supports our results on the relationship between the PE and sequence evolution.

#### IV. CONCLUSIONS

It is well known that the hydrophobicity is a major determinant of protein stability and evolution. We have shown that, among several hydrophathy scales, the optimized interactivity scale (Bastolla et al., 2004b) is the one best correlated with various thermodynamic and genomic quantities.

The influence of the hydrophobicity on protein stability has two sides: On the one hand, the more hydrophobic a protein is, the more stable is with respect to unfolding; on the other hand it is less stable with respect to misfolding, so that a careful tuning of the hydrophobic content is needed (Bastolla et al., 2004a). Close to the optimal hydrophobicity, small variations have complex effects that might reduce their impact on fitness. This is probably the reason why the mutational bias is able to influence hydrophobicity and hence protein folding thermodynamics. Large variations of the mean hydrophobicity, however, are not tolerated in the course of evolution.

In order to achieve folding stability, we have predicted that the hydrophobicity should be distributed within the protein sequence in a site-specific manner, which is mainly influenced by a site-specific indicator – the principal eigenvector of the contact matrix (PE). From the hypothesis that the correlation between the hydrophobicity and the PE is the only condition imposed by folding stability on sequence evolution, we predicted analytically site-specific amino acid distributions to be of Boltzmann type, in agreement with simulations of the SCN model of protein evolution and with structural alignments of

sites with equivalent PE taken from the PDB.

Finally, we have discussed how simple mutational models improve the fit between predicted and observed site-specific distributions. Interestingly, the model that provides the best fit is also one with almost the lowest rate of rejected mutations.

This observation is consistent with the suggestions that error correction systems might have evolved to minimize the impact of mutations on protein stability.

- Abkevich, V.I., Gutin, A.M., Shakhnovich, E.I. 1994. Free energy landscapes for protein folding kinetics - intermediates, traps and multiple pathways in theory and lattice model simulations. *J. Chem. Phys.* **101**:6052-6062.
- Babajide, A., Hofacker, I.L., Sippl, M.J., Stadler, P.F. 1997. Neutral networks in protein space. *Fol. Des.* **2**:261-269.
- Bastolla, U., Frauenkron, H., Gerstner, E., Grassberger, P., Nadler, W. 1998. Testing a new Monte Carlo algorithm for protein folding. *Proteins* **32**:52-66.
- Bastolla, U., Vendruscolo, M., Roman, H.E. 1999. Neutral evolution of model proteins: Diffusion in sequence space and overdispersion. *J. Theor. Biol.* **200**:49-64.
- Bastolla, U., Vendruscolo, M., Knapp, E.W. 2000. A statistical mechanical method to optimize energy parameters for protein folding. *Proc. Natl. Acad. Sci. USA* **97**:3977-3981.
- Bastolla, U., Knapp, E.W., Vendruscolo, M. 2001. How to guarantee optimal stability for most protein native structures in the Protein Data Bank. *Proteins* **44**:79-96.
- Bastolla, U., Porto, M., Roman, H.E., Vendruscolo, M. 2002. Lack of self-averaging in neutral evolution of proteins. *Phys. Rev. Lett.* **89**:208101/1-208101/4.
- Bastolla, U., Porto, M., Roman, H.E., Vendruscolo, M. 2003a. Connectivity of neutral networks, overdispersion and structural conservation in protein evolution. *J. Mol. Evol.* **56**:243-254.
- Bastolla, U., Porto, M., Roman, H.E., Vendruscolo, M. 2003b. Statistical properties of neutral evolution. *J. Mol. Evol.* **57**:S103-S119.
- Bastolla, U., Moya, A., Viguera, E. van Ham, R.C.H.J. 2004a. Genomic determinants of protein folding thermodynamics. *J. Mol. Biol.*, in print.
- Bastolla, U., Porto, M., Roman, H.E., Vendruscolo, M. 2004b. The principal eigenvector of contact matrices and hydrophobicity profiles in proteins. *Proteins*, in print.
- Bateman, A., Birney, E., Durbin, R., Eddy, S.R., Howe, K.L., Sonnhammer, E.L.L. 2000. The PFAM contribution to the annual NAR database issue. *Nucl. Ac. Res.* **28**:263-266.
- Bernardi, G., Bernardi, G. 1986. Compositional constraints and genome evolution. *J. Mol. Evol.* **24**:1-11.
- Bornberg-Bauer, E. 1997. How are model protein structures distributed in sequence space? *Biophys. J.* **73**:2393-2403;
- Bornberg-Bauer, E., Chan, H.S. 1999. Modeling evolutionary landscapes: Mutational stability, topology, and superfunnels in sequence space. *Proc. Natl. Acad. Sci. USA* **96**:10689-10694.
- Bryngelson J.D., Wolynes, P.G. 1987. Spin-glasses and the statistical-mechanics of protein folding. *Proc. Natl. Acad. Sci. USA* **84**:7524-7528.
- Bussemaker, H.J., Thirumalai, D., Bhattacharjee, J.K. 1997. Thermodynamic stability of folded proteins against mutations. *Phys. Rev. Lett.* **79**:3530-3533.
- Casari G., Sippl, M.J. 1992. Structure-derived hydrophobic potential. Hydrophobic potential derived from X-ray structures of globular proteins is able to identify native folds. *J. Mol. Biol.* **224**:725-732.
- Dokholyan, N.V., Shakhnovich, E.I. 2001. Understanding hierarchical protein evolution from first principles. *J. Mol. Biol.* **312**:289-307.
- Dokholyan, N.V., Mirny, L.A., Shakhnovich, E.I. 2002. Understanding conserved amino acids in proteins. *Physica A* **314**:600-606.
- Fares, M.A., Moya, A., Barrio, E. 2004. GroEL and the maintenance of bacterial endosymbiosis. *Trends in Genetics* **20**:413-416.
- Fauchere, J.L., Pliska, V. 1983. Hydrophobic parameters of amino acid side chain from the partitioning N-acetyl amino acid amides. *Eur. J. Med. Chem.* **18**:369-375.
- Felsenstein, J. 1981. Evolutionary trees from DNA sequences: A maximum likelihood approach. *J. Mol. Evol.* **17**:368-376.
- Fontana, W., Schuster, P. 1998. Continuity in evolution: On the nature of transitions. *Science* **280**:1451-1455.
- Fornasari, M.S., Parisi, G., Echave, J. 2002. Site-specific amino acid replacement matrices from structurally constrained protein evolution simulations. *Mol. Biol. Evol.* **19**:352-356.
- Goldstein, R.A., Luthey-Schulten Z.A., Wolynes, P.G. 1992. Optimal protein-folding codes from spin-glass theory. *Proc. Natl. Acad. Sci. USA* **89**:4918-4922.
- Govindarajan, S., Goldstein, R.A. 1998. On the thermodynamic hypothesis of protein folding. *Proc. Natl. Acad. Sci. USA* **95**:5545-5549.
- Gromiha, M.M., Oobatake, M., Kono, H., Uedaira, H., Sarai, A. 1999. Role of structural and sequence information in the prediction of protein stability changes: comparison between buried and partially buried mutations. *Prot. Eng.* **12**:549-555.
- Gu, X., Hewett-Emmett, D., Li, W.H. 1998. Directional mutational pressure affects the amino acid composition and hydrophobicity of proteins in bacteria. *Genetica* **102-103**:383-391.
- Gueoris, R., Nielsen, J.E., Serrano, L. 2002. Predicting changes in the stability of proteins and protein complexes: A study of more than 1000 mutations. *J. Mol. Biol.* **320**:369-387.
- Gutin, A.M., Abkevich, V.I., Shakhnovich, E.I. 1995. Evolution-like selection of fast-folding model proteins. *Proc. Natl. Acad. Sci. USA* **92**:1282-1286.
- Halpern, A.L., Bruno, W.J. 1998. Evolutionary distances for protein-coding sequences: modeling site-specific residue frequencies. *Mol. Biol. Evol.* **15**:910-917.
- Hartl, F.U., Hayer-Hartl, M. 2002. Protein folding - Molecular chaperones in the cytosol: from nascent chain to folded protein. *Science* **295**:1852-1858.
- Henikoff, S., Henikoff, J.G. 1992. Amino acid substitution matrices from protein blocks. *Proc. Natl. Acad. Sci. USA* **89**:10915-10919.
- Hobohm, U., Sander, C. 1994. Enlarged representative set of protein structure. *Protein Sci* **3**:522-524.
- Holm, L., Sander, C. 1996. Mapping the protein universe. *Science* **273**:595-602.
- Huynen, M.A., Stadler, P.F., Fontana, W. 1996. Smoothness within ruggedness: The role of neutrality in adaptation. *Proc. Natl. Acad. Sci. USA* **93**:397-401.
- Jayasinghe S, Hristova, K., White, S.H. 2001. Energetics, stability, and prediction of transmembrane helices. *J. Mol. Biol.* **312**:927-934.
- Kinjo, A.R., Nishikawa, K. 2004. Eigenvalue analysis of amino acid substitution matrices reveal a sharp transition of the mode

- of sequence conservation in proteins. *Bioinformatics* **20**:2504-2508.
- Klimov, D.K., Thirumalai, D. 1996. Factors governing the foldability of proteins. *Proteins* **26**:411-441.
- Koshi, J.M., Goldstein, R.A. 1998. Models of natural mutation including site heterogeneity. *Proteins* **32**:289-295.
- Koshi, J.M., Mindell, D.P., Goldstein, R.A. 1999. Using physical-chemistry based substitution models in phylogenetic analysis of HIV-1 subtypes. *Mol. Biol. Evol.* **16**:173-179.
- Kyte, J., Doolittle, R.F. 1982. A simple method for displaying the hydropathic character of a protein. *J. Mol. Biol.* **157**:105-132.
- Levitt, M. 1976. A simplified representation of protein conformations for rapid simulation of protein folding. *J. Mol. Biol.* **104**:59-107.
- Li, H., Tang, C., Wingreen, N.S. 1997. Nature of driving force for protein folding: A result from analyzing the statistical potential. *Phys. Rev. Lett.* **79**:765-768.
- Liò, P., Goldman, N. 1998. Models of molecular evolution and phylogeny. *Genome Res.* **8**:1233-1244.
- Lobry, J.R. 1997. Influence of genomic G+C content on average amino-acid composition of proteins from 59 bacterial species. *Gene* **205**:309-316.
- Manavalan, P., Ponnuswamy, P.K. 1978. Hydrophobic character of amino acid residues in globular proteins. *Nature* **275**:673-674.
- Mirny, L.A., Abkevich, V.I., Shakhnovich, E.I. 1998. How evolution makes proteins fold quickly. *Proc. Natl. Acad. Sci. USA* **95**:4976-81.
- Nei, M., Kumar, S., 2000. *Molecular evolution and phylogenetics*. Oxford Univ. Press.
- Ohta, T. 1976. Role of very slightly deleterious mutations in molecular evolution and polymorphism. *Theor. Pop. Biol.* **10**:254-275.
- Palliser, C.C., Parry, D.A. 2001. Quantitative comparison of the ability of hydropathy scales to recognize surface beta-strands in proteins. *Proteins* **42**:243-255.
- Parisi, G., Echave, J. 2001. Structural constraints and emergence of sequence patterns in protein evolution. *Mol. Biol. Evol.* **18**:750-756.
- Porto, M., Bastolla, U., Roman, H.E., Vendruscolo, M. 2004a. Reconstruction of protein structures from a vectorial representation. *Phys. Rev. Lett.* **92**:218101/1-218101/4.
- Porto, M., Roman, H.E., Vendruscolo, M., Bastolla, U. 2004b. Prediction of site-specific amino acid distributions and limits of divergent evolutionary changes in protein sequences. *Mol. Biol. Evol.*, in print.
- Roseman, M.A. 1988. Hydrophobicity of polar amino-acid side chains is markedly reduced by flanking peptide bonds. *J. Mol. Biol.* **200**:513-522.
- Schuster, P., Fontana, W., Stadler, P.F., Hofacker, I.L. 1994. From sequences to shapes and back – A case-study in RNA secondary structures. *Proc. R. Soc. London B* **255**:279-284;
- Sueoka, N. 1961. Correlation between base composition of the deoxyribonucleic acid and amino acid composition of proteins. *Proc. Natl. Acad. Sci. USA* **47**:469-478.
- Tiana, G., Broglia, R.A., Roman, H.E., Vigezzi, E., Shakhnovich, E.I. 1998. Folding and misfolding of designed proteinlike chains with mutations. *J. Chem. Phys.* **108**:757-761.
- Thorne, J.L. 2000. Models of protein sequence evolution and their applications. *Curr. Opin. Genet. Dev.* **10**:602-605.
- Uversky, V.N. 2002. Natively unfolded proteins: a point where biology waits for physics. *Protein Sci.* **11**:739-756.
- Uversky, V.N. 2002. Cracking the folding code. Why do some proteins adopt partially folded conformations, whereas other don't? *FEBS Lett.* **514**:181-183.
- White, S.H. 1992. Amino acid preferences of small proteins. Implications for protein stability and evolution. *J. Mol. Biol.* **227**:991-995.
- Zhou, H., Zhou, Y. 2004. Quantifying the effect of burial of amino acid residues on protein stability. *Proteins* **54**:315-322.